AN EFFICIENT MAXIMUM-POWER-POINT-TRACKING CONTROLLER FOR GRID-CONNECTED PHOTOVOLTAIC ENERGY CONVERSION SYSTEM

Marcelo G. Molina[1] Domingo H. Pontoriero[2] Pedro E. Mercado[1]
[1] Argentinean National Research Council for Science and Technology – CONICET
[1, 2] National University of San Juan – UNSJ
Institute of Electrical Energy – IEE
Av. Libertador Gral. San Martín Oeste 1109 – J5400ARL – San Juan – Argentina
mgmolina@iee.unsj.edu.ar – http://www.iee-unsj.org

***Abstract* – This paper investigates the effectiveness of the "Perturbation and Observation" (P&O) method and "Incremental Conductance" (IncCond) method through simulations carried out by using SimPowerSystems of MATLAB/Simulink®. Both the steady-state and transient characteristics of each control algorithm are fully analyzed and compared by using a proposed performance index. Finally, a new MPPT control algorithm based on an enhanced incremental conductance method is proposed in order to improve the efficiency of the PV power generation system at different climatic and load conditions. An adaptive duty cycle perturbation step size is made dependent on the sensitivity of the PV array power to the previous perturbation in order to obtain a fast dynamic response and accurate tracking of the MPP. Digital simulations and experimental results demonstrate the superior performance of the proposed technique.**

***Keywords* – Adaptive Duty Cycle Algorithm, Boost Converter, Digital Signal Processor, Maximum Power Point Tracker, Photovoltaic System.**

I. INTRODUCTION

The world depletion of fossil energy and the environmental pollution have impelled during decades the development of renewable energies. This situation has become worst in the last years due to the global climate warming increase taken place by greenhouse gas emissions, primarily carbon dioxide (CO2), and the rupture of the ozone layer by Freon gas. In this way, the need of having available sustainable energy systems for replacing conventional ones requires the development of structures of energy supply based mostly on clean and renewable sources.

At present, photovoltaic generation is assuming increased importance as a renewable source because of distinctive advantages such as simplicity of allocation, high dependability, absence of fuel cost, low maintenance and lack of noise and wear due to the absence of moving parts. Furthermore, the solar energy characterizes a clean, pollution-free and inexhaustible energy source. In addition to this factors are the continuous decrease of investment cost of solar modules and the increase of their efficiency in the energy conversion. However, these last two factors limit the implementation of PV systems. In photovoltaic systems, the PV panel represents 57 % of the total investment cost of the system, and the battery storage system corresponds to 30 % of the cost. The rest of the components of the system, such as the power electronic devices and the control systems contribute only with the remaining 13 % of the total cost.

The high costs of photovoltaic arrays impose the necessity of being constantly operating the PV system near the maximum power point (MPP) independently of the climatic conditions and of the load voltage. In this way, the relationship between maximum power and investment cost of PV arrays has to be maximized. As is well-known, the maximum power provided by a solar cell depends on the temperature and the solar radiation (also called insolation), which are unpredictable climatic factors, in such a way that the continuous tracking of the MPP needs to be implemented. Furthermore, for grid-connected PV systems it is required the use of high efficiency power converters for injecting the active power into the utility electric system aiming at lessening stress on the overall system and improving the power quality among others factors.

For years, different control techniques have been developed in order to provide MPP tracking [1]–[10]. Among them, some methods control the PV module characteristics to match particular load conditions [1]–[4]; in addition integrated PV-MPPT with soft switching to obtain the optimum efficiency was proposed [5]. Moreover, neural networks for MPP tracking and fuzzy logic control algorithms were applied [6]–[8]. Another type of MPP tracking is based on continuous adjustment of the load seen by the PV array in order to match with its MPP. This technique can be achieved by means of discrete elements and sensors; however, the use of microprocessors or digital signal processors (DSP) has the additional advantages of control flexibility and easiness of application with different types of PV arrays [9]–[10]. The power efficiency of this technique relies on the software algorithm that tracks the MPP by measuring various array quantities (voltage, current and power).

Among all the techniques previously described, digital controller and DSP-based ones have largely drawn the attention of researchers due to the good combination of flexibility, accuracy and simplicity. From these last, two MPPT algorithms stands out because of their usefulness, being: "Perturbation and Observation" (P&O) method [10] and "Incremental Conductance" (IncCond) method [11].

Based on these considerations, this paper investigates in detail the effectiveness of this two control algorithms through

Manuscript received September 10, 2006; revised December, 19, 2006 and May 15, 2007. Recommended by the Editors of the Special Section D. C. Martins and F. L. M. Antunes.

simulations carried out by using SimPowerSystems of MATLAB/Simulink®. Both the steady-state and transient characteristics of each control algorithm are fully analyzed and compared by using a proposed performance index that takes into account these two features. Finally, a new MPPT control algorithm based on an enhanced incremental conductance method is proposed in order to improve the efficiency of the PV power generation system at different climatic and load conditions. An adaptive duty cycle perturbation step size is made dependent on the sensitivity of the PV array power to the previous perturbation in order to obtain a fast dynamic response and the accurate tracking of the MPP. Digital simulations and experimental results demonstrate the higher performance of the proposed technique above the others.

II. MODEL OF THE PV CELL/ARRAY

The building block of the PV array is the solar cell, which is basically a p–n semiconductor junction that directly converts solar radiation into dc current using the photovoltaic effect. Figure 1 depicts the well-known equivalent circuit of the solar cell composed of a light generated current source, a diode representing the nonlinear impedance of the p-n junction, and series and parallel intrinsic resistances [12].

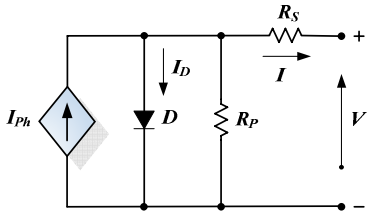

Fig. 1. Equivalent circuit of a PV cell.

PV cells are grouped together in larger units known as PV modules or arrays, which are combined in series and parallel to provide the desired output voltage and current. The equivalent circuit for the solar cells arranged in N_p – parallel and N_s – series is shown in Figure 2. The mathematical equation for the current and voltage of this PV generator becomes as in (1):

$$I_A = N_P I_{Ph} - N_P I_{RS}\left\{\exp\left[\frac{q}{AkT}\left(\frac{V_A}{N_S}+\frac{I_A R_S}{N_P}\right)\right]-1\right\} - \frac{N_P}{R_P}\left(\frac{V_A}{N_S}+\frac{I_A R_S}{N_P}\right) \quad (1)$$

Where:

I_A: - PV array output current.
V_A: - PV array output voltage.
I_{Ph}: - Solar cell photocurrent.
I_{RS}: - Cell reverse saturation current.
q: - Charge of an electron, $1.60217733 \cdot 10^{-19}$ Cb.
A: - P-N junction ideality factor, between 1 and 5.
k: - Boltzmann's constant, $1.380658 \cdot 10^{-23}$ J/K.
T: - Solar cell temperature in K.
R_S: - Cell intrinsic series resistance.
R_P: - Cell intrinsic parallel resistance.

The solar cell reverse saturation current I_{RS} varies with temperature according to the following equation:

$$I_{RS} = I_{RR}\left[\frac{T}{T_R}\right]^3 \exp\left[\frac{qE_G}{Ak}\left(\frac{1}{T_R}-\frac{1}{T}\right)\right] \quad (2)$$

Where:

T_R: - Cell reference temperature in K.
I_{RR}: - Cell reverse saturation current at T_R.
E_G: - Band-gap energy of the cell semiconductor.

The photocurrent I_{Ph} depends on the solar radiation and the cell temperature as follows:

$$I_{Ph} = \left[I_{SC} + k_T\left(T - T_R\right)\right]\frac{S}{1000} \quad (3)$$

Where:

I_{SC}: - Cell short-circuit current at reference temperature and radiation
k_T: - Short-circuit current temperature coefficient
S: - Solar radiation in W/m^2

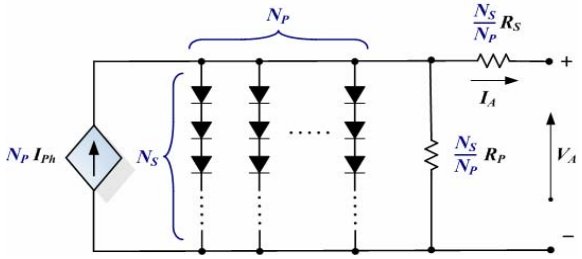

Fig. 2. Equivalent circuit of a PV array.

As can be clearly derived from (1) to (3), the PV array exhibits a highly nonlinear radiation and temperature-dependent *I–V* and *P–V* characteristic curve, which are illustrated in Figures 3 and 4 respectively for different levels of solar radiation and cell temperature. By making step variations in the solar radiation S and the cell temperature T in (1) to (3), the *I-V* and the *P-V* characteristics of the PV array were simulated by using Simulink environment [13] for a BP 250/1 (BP Solar), 50 W high efficiency monocrystalline PV module, being the characteristics presented in Table I for simulated and experimental data (standard test conditions of insolation and cell temperature: 1000 W/m^2 and 25ºC).

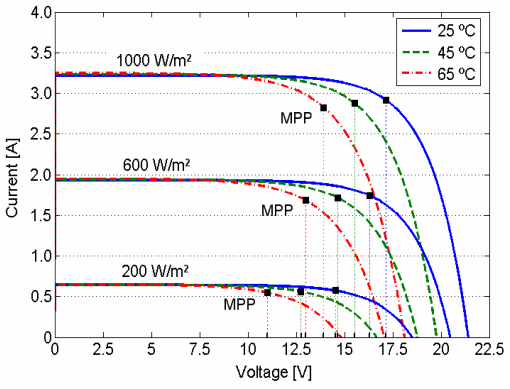

Fig. 3. Simulated *I-V* characteristic of a BP 250/1 PV module for various levels of solar radiation.

As can be noted from Figure 3, the PV array has an MPP which splits the output *I-V* characteristic curve into two parts: the left part is defined as the current source region in which the output current approximates to a constant, and the right part is the voltage source region in which the output

voltage hardly changes. Since the MPP changes with variations in radiation and temperature, a continuous adjustment of the array terminal voltage is required for providing maximum power to the load. In addition, by considering that for grid-connected applications the loads supplied by PV systems operate with constant voltage, it is necessary to track the MPP of the solar cell regardless the load voltage. From Figure 4 it can be clearly derived the optimum operation point for the PV system, i.e. the MPP, at different radiation and temperature conditions.

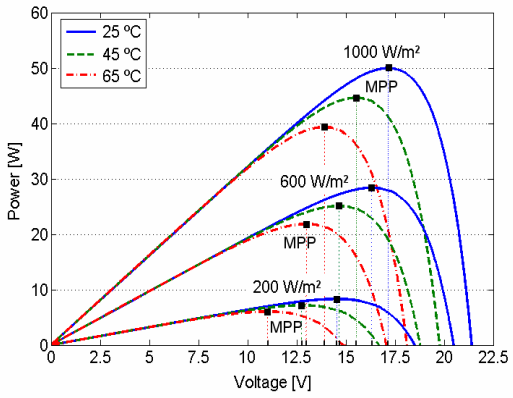

Fig. 4. Simulated *P-V* characteristic of a BP 250/1 PV module for various levels of solar radiation.

TABLE I
BP 250/1 module data comparison (1000 W/m^2, 25ºC)

BP 250 Module	Catalogue Data	Experimental Results	Simulation Results
Maximum power [W]	50	49.93	49.71
Voltage at MPP [V]	17	17.15	17.23
Current at MPP [A]	2.94	2.91	2.89
Short-circuit Current A]	3.22	3.2	3.18
Open-circuit Voltage [V]	21.20	21.32	21.4

A. Influence of the Solar Radiation

Figures 3 and 4 permit to examine the influence of the solar radiation on the output *I-V* and *P-V* characteristics, for a specific temperature of the solar cell. The MPP varies according to the radiation changes, modifying the voltage at MPP over a 2.3 V range from 200 to 1000 W/m^2. Thus, for an operation in the lower boundary of the MPP voltage at minimum radiation, i.e. at a voltage of 14.5 V (200 W/m^2, 25 ºC) and considering the worst case of a sudden change to the maximum radiation (200 to 1000 W/m^2), then the voltage should be modified to 16.9 V for tracking the MPP. Otherwise the electric power wasted should be about 2.3 W, which is almost 5 % of the solar-array rated power.

B. Influence of the Cell Temperature

As in the previous analysis, the influence of the cell temperature for a specific solar radiation can be performed by inspecting Figures 2 and 3. The MPP varies according to the temperature changes, modifying the voltage at MPP over a 3.5 V range from 25 to 65 ºC at 1000 W/m^2. Thus, for an operation in the higher boundary of the MPP voltage at minimum temperature, i.e. at a voltage of 17.3 V (1 kW/m^2, 25 ºC) and considering the worst case of a sudden change to the maximum cell temperature (25 to 65 ºC), then the voltage should be modified to 13.7 V for tracking the MPP. If this condition is not fulfilled, the electric power wasted should be about 11.3 W, which is nearly 22.6 % of the PV rated power.

From the previous analysis at actual operating conditions, the magnitude of both climatic factors on the efficiency of the PV system has been laid down. As demonstrated, it is therefore desirable to keep the PV module temperature as low as possible in order to draw the maximum power from the module. Cell temperature shows to have more influence on the position of the MPP and then on the power efficiency of the PV system than the solar radiation, but experimental results reveal that the speed of changes are by far higher for the case of the solar radiation than for the cell temperature.

III. DC-DC BOOST CONVERTER

For grid-connected PV applications, two hardware topologies for MPPT have been mostly studied worldwide, known as one-stage and two-stage PV systems. In this work, it was selected the two-stage PV energy conversion system because it offers an additional degree of freedom in the operation of the system when compared with the one-stage configuration. Generally, it is achieved at the expense of slightly decreasing the global efficiency of the overall system because of connecting two cascade stages. Hence, by including a dc-dc converter or chopper between the PV array and the power inverter linked to the electric grid, as shown in Figure 5, various control objectives are possible to pursue simultaneously with the PV system operation. Considering the integration of the PV array with the voltage source inverter (VSI) presented in [14], the performance of the grid-connected PV-MPPT system is studied henceforth.

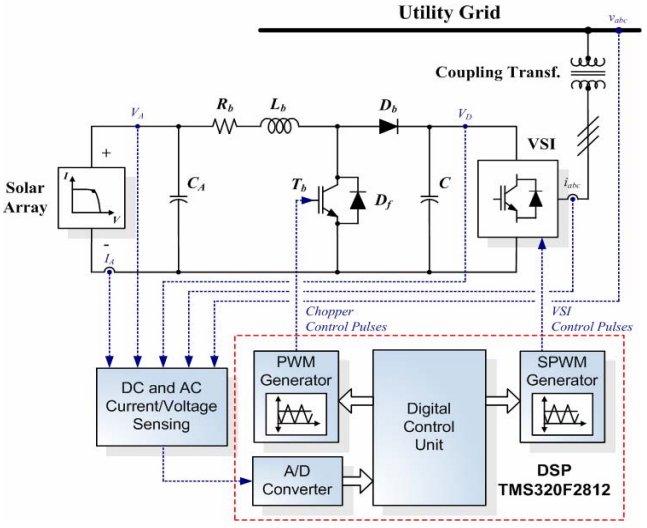

Fig. 5. Schematic of the unidirectional boost dc-dc converter as a part of the three-phase grid-connected PV system.

The intermediate dc-dc converter is built with an Insulated Gate Bipolar Transistor (IGBT) as main power switch T_b in a standard unidirectional boost topology that employs an energy-storage inductor L_b, a rectifier diode D_b and a voltage smoothing capacitor C. The converter is linked to the PV system composed of four modules BP 250/1 connected in

series (P_{max}=200 W), with a filter capacitor C_A for reducing the high frequency ripple generated by the transistor switchings. The dc-dc converter output is connected to the dc bus of the VSI as depicted in Figure 5.

Figure 6 illustrates the simplified control scheme of the overall grid-connected PV system. The main purpose of this controller is to transfer the maximum solar array power into the utility grid. This objective is fulfilled by using the output power signal generated by the MPP tracker (P_r) for yielding a direct current reference (i_{dr}*) for the VSI current controller. An additional contribution to the direct current reference (i_{dr}') is applied in order to regulate the dc bus voltage (V_d) at a constant value via a PI controller. This is achieved by forcing a small active power exchange with the electric grid for compensating the transformer winding and VSI IGBTs losses. As reactive power exchange is not considered in this case, i_{dr} is set to 0. It is to be noted that a simplified stated-space model of the VSI in the *dq* frame, which is detailed in depth in [14], is employed for generating the control pulses for the VSI IGBTs.

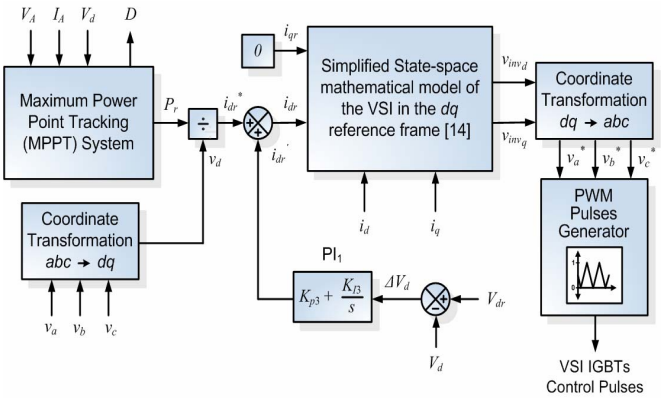

Fig. 6. Control of the three-phase grid-connected PV system.

The dc-dc converter produces a chopped output voltage and therefore controls the average dc voltage relation between its input and output aiming at continuously matching the characteristic of the PV generator to the equivalent impedance presented by the dc bus of the VSI. The steady-state voltage and current relations of the boost converter operating in continuous conduction mode are stated by (4) and (5) as follows:

$$V_D = \frac{V_A}{(1-D)} \tag{4}$$

$$I_D = \eta_b \,(1-D)\, I_A \tag{5}$$

Where:

η_b: - Efficiency of the boost converter.
D: - Dc-dc converter duty ratio.
I_A: - PV array output current.
V_A: - PV array output voltage.
I_D: - Dc bus current (inverter side).
V_D: - Dc bus voltage (inverter side).

The power efficiency η_b of the dc-dc converter exhibits a nonlinear characteristic relative to the output power injected into the dc bus of the inverter. This characteristic is also applicable to the output dc current. In Figure 7, the actual steady-state efficiency of the chopper built into laboratory is shown, which was measured with the PV array at maximum solar radiation (1 kW/m^2) and temperature of 25ºC.

The power extracted by the boost converter from the PV array, P_A can be expressed as:

$$P_A = \frac{{V_A}^2}{\eta_b (1-D)^2 \, Z_{EqD}} \tag{6}$$

Where:

Z_{EqD}: - Dc bus equivalent impedance

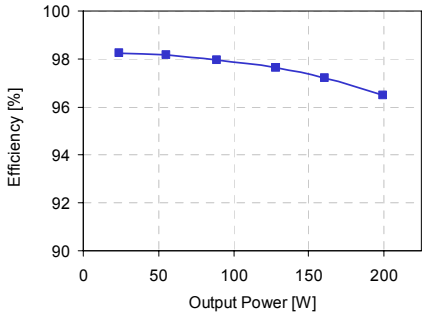

Fig. 7. Actual efficiency of the dc-dc boost converter for different levels of output power (PV at 1kW/m^2 and 25ºC).

From the above expression the array power P_A depends on the converter duty ratio and the impedance presented by the dc bus of the inverter. By considering constant the dc bus voltage (V_d), as previously expressed, it is possible to control the maximum power to be drawn from the PV system for given environmental conditions simply by varying the duty cycle *D*. In this way, for the PV system employed in this work (four modules BP 250/1) with specifications and components summarized in Table III, the *I-V* characteristic curve can be tested by making small changes in the duty cycle for various levels of temperature and solar radiation, as depicted in Figure 8.

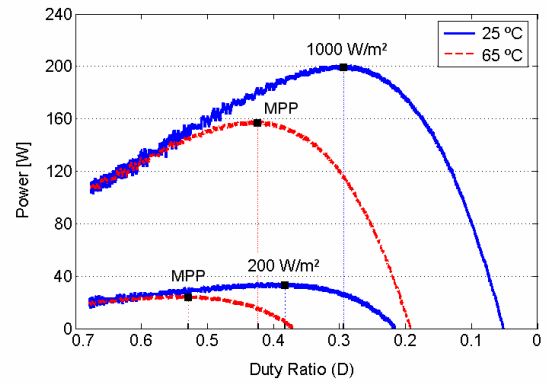

Fig. 8. MPP tracking process with duty ratio.

IV. MPPT CONTROL ALGORITHMS

Maximum power point tracking means that the PV system is always supposed to operate at maximum output voltage/current rating. Simulation of the PV array provides a flexible means of analysing and comparing the performance of different MPPT algorithms when operated under specific climatic conditions. Henceforth, most classical MPPT control methods are discussed, that is to say "Perturbation and Observation" (P&O) method and "Incremental Conductance" (IncCond) method.

A. Perturbation and Observation Algorithm

P&O algorithms are widely used because of their simple structure and the few measured variables which are necessary, as depicted in Figure 9. They operate by constantly perturbing (i.e. increasing or decreasing) the array terminal voltage V_A via the dc-dc converter duty cycle and comparing the actual PV output power P_A with the previous perturbation sample P_P. If the power is increasing, the perturbation will continue in the same direction in the following cycle, otherwise the perturbation direction will be inverted. This means the array terminal voltage is perturbed every MPPT cycle at sample intervals T_S; therefore when the MPP is reached, the P&O algorithm will oscillate around this point resulting in a loss of PV power, especially in cases of constant or slowly varying atmospheric conditions. On the other hand, in cases of rapidly changing environment conditions, e.g. as a result of moving clouds, it was verified that the P&O algorithm deviates from the MPP [11]. The MPPT algorithm can be confused due to the fact that it is not able to distinguish the variations of the PV array output power caused by the duty cycle from those ones caused by the solar radiation deviation.

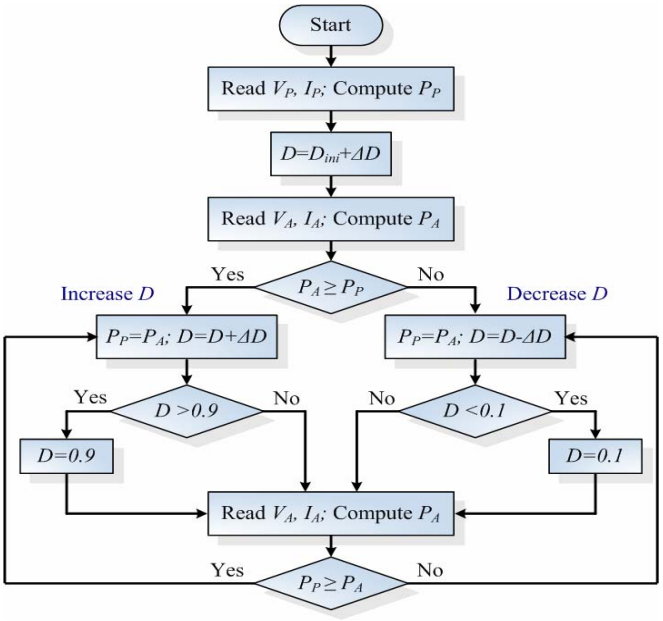

Fig. 9. Flowchart for the P&O MPPT algorithm.

As described in [15], it is shown that the negative effects associated to such a drawback can be significantly reduced if the magnitude of the duty cycle perturbations ΔD and the sampling interval T_S are customized to the dynamic behaviour of the specific dc-dc converter employed to realize the P&O MPPT algorithm.

B. Incremental Conductance Algorithm

In order to solve the above mentioned problems of P&O methods, the IncCond algorithm was developed by [11] which tracks the MPP of the PV array by using a different procedure. The method is based on the fact that at the MPP, the derivative of the PV output power with respect to the PV voltage is zero. Thus, the PV voltage can be regulated relative to the voltage at the MPP by measuring the incremental conductance, dI/dV and conductance, I/V.

The algorithm, which is summarized in Figure 10, begins its cycle by obtaining actual (A) and previous (P) values of I and V, i.e. I_A, V_A and I_P, V_P respectively; then by using these measurements, the incremental changes are approximated as: $dI \approx I_A - I_P$ and $dV \approx V_A - V_P$. The major comparison is carried out by comparing dI/dV against $-I/V$, as emerges from (7).

$$\frac{dP}{dV} = \frac{d(IV)}{dV} = I + V\frac{dI}{dV} \approx I + V\frac{\Delta I}{\Delta V} \tag{7}$$

$$\frac{dP}{dV} = 0 \qquad \text{at the MPP,} \tag{8}$$

$$\frac{dP}{dV} > 0 \quad \text{to the left of the MPP,} \tag{9}$$

$$\frac{dP}{dV} < 0 \quad \text{to the right of the MPP,} \tag{10}$$

The result of computing (7) through (10), will determine the direction of the required change in the control voltage variable and therefore the duty cycle so as to move the PV voltage towards the MPP.

This algorithm has the advantage of reducing to minimum the oscillations around the MPP in steady-state unlike the P&O algorithm. However, the drawback of this algorithm is the complexity for designing the controller. Although, this disadvantage is not an issue for current grid-connected PV applications that implements all the control schemes through a digital controller or a DSP.

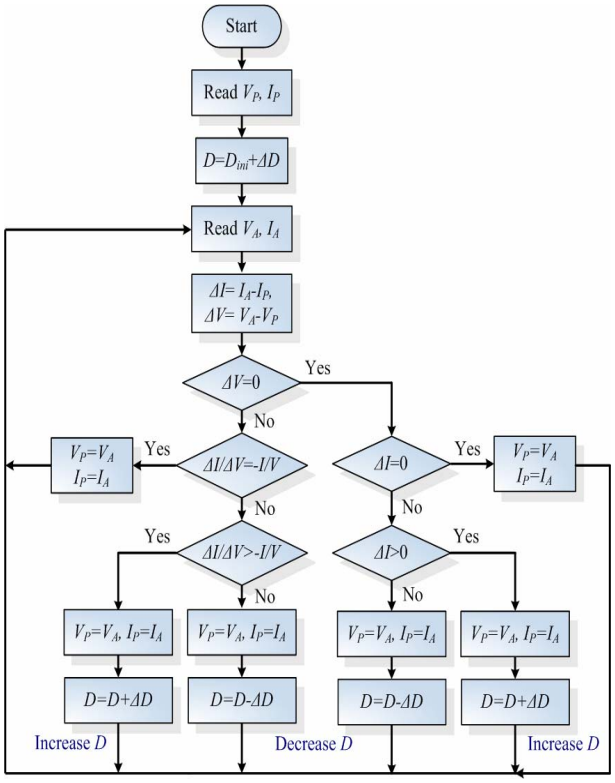

Fig. 10. Flowchart for the IncCond MPPT algorithm.

C. Proposed MPPT Algorithm

The proposed MPPT system consists of an improved Incremental Conductance Algorithm which uses adaptive variable step sizes (ΔD) applied to the duty cycle of the dc-dc converter. The aim of these modifications over the

conventional IncCond method is to achieve a fast dynamic response and accurate tracking of the MPP under rapidly changing environmental conditions. The process of the proposed MPPT algorithm is depicted in the flowchart presented in Fig. 11. The size of the step ΔD is made dependent on the sensitivity of the PV power to the previous perturbation, through the term δ as expressed in (11).

$$\delta = \frac{dP}{P_A} \approx \frac{\Delta P}{P_A} \approx \frac{P_A - P_P}{P_A} \approx \frac{\left(V_A I_A - V_P I_P\right)}{P_A} \tag{11}$$

According to the sign of the perturbation, and therefore to the sign of δ, the duty cycle of the dc-dc converter is computed as settled in (12) and (13),

$$\Delta D = k_1\, \delta \quad \text{for } \Delta P>0, \tag{12}$$

$$\Delta D = -k_2\, \delta \quad \text{for } \Delta P<0, \tag{13}$$

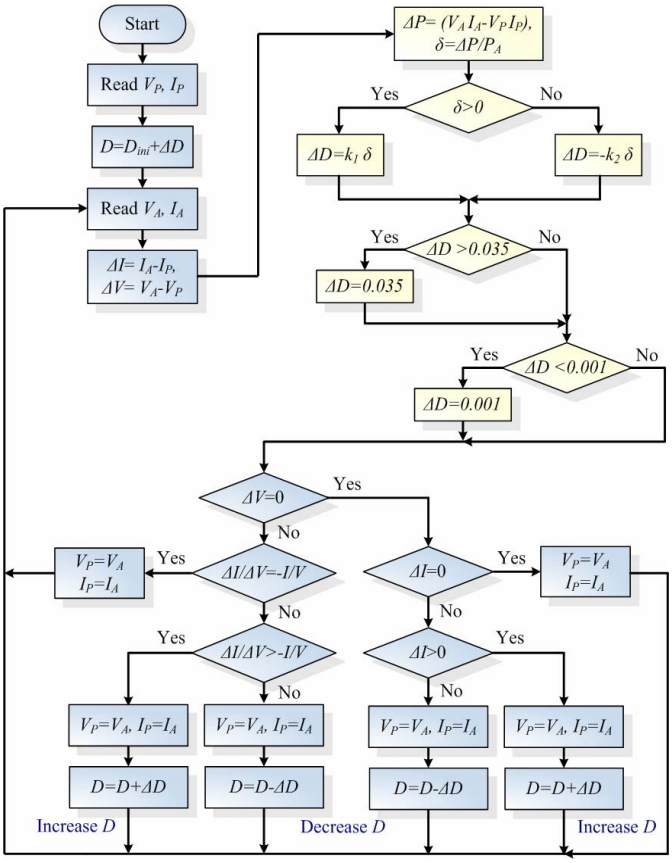

Fig. 11. Flowchart for the Proposed MPPT algorithm.

The additional terms k_1 and k_2, are included in order to allow the sensitivity to be enhanced for accomplishing both rapid action toward the MPP tracking in case of a large change in the characteristic curve of the PV system and to assist accurately in converging to the true MPP for steady-state conditions. If the step size of the duty cycle, ΔD is very large as a result of a big change in climatic conditions, the needs of limiting this quantity in order to avoid overshooting in the MPP tracking arises. In the same way, the minimum size of ΔD must be limited to the smaller value that permits to obtain minimum steady-state oscillation around the MPP without introducing instability and being reachable with the controller or DSP used for implementing the algorithm. The values of k_1 and k_2 are found by trial and error, customized for the dynamic behaviour of the employed boost converter. Since the converter exhibits a slightly different dynamic behaviour during a positive δ (increase of ΔD) when compared to the negative sensibility (decrease of ΔD), two different values are proposed for k_1 and k_2, aiming at making similar both dynamic responses of the power conditioning system.

V. SIMULATIONS AND EXPERIMENTAL RESULTS

A. Selection of Perturbation Step-Size

The MPPT algorithm efficiency is directly related to the selection of the duty cycle perturbations ΔD and the sampling interval T_S, as well as the intrinsic effectiveness of the method. It is also significant to note that the algorithm influences not only the MPPT efficiency but also the dc-dc boost converter efficiency. For a given sampling interval, the larger the perturbation step the faster the maximum power that can be drawn from the PV array. However, the larger the perturbation step-size, the larger are the intrinsic oscillations around the MPP in steady-state. These oscillations reduce the effectiveness of the PV energy system. On the other hand, a smaller perturbation step-size reduces the magnitude of oscillations around the MPP in steady-state and increases the energy conversion effectiveness once the MPP has been achieved. However, it would lead to slow response under rapidly changing environmental conditions. Consequently, there is a trade-off between fast MPP tracking and power error in selecting the appropriate size of the perturbation step.

B. Digital Simulation Results

Both the steady-state and transient characteristics of all MPPT control algorithms previously described are studied. In this sense, in order to compare the performance of these algorithms, an evaluation based on the efficiency of each method in drawing the maximum energy from the PV array is adopted. The energy efficiency $\eta_{e,PV}$ of the algorithms relative to the theoretical maximum power available from the PV array, P_{MPP} can be computed by using (14) as follows:

$$\eta_{e,PV} = \frac{\int_{t_1}^{t_2} P_A\, dt}{\int_{t_1}^{t_2} P_{MPP}\, dt} \tag{14}$$

In the same way, for the case of the dc-dc boost converter, the energy efficiency $\eta_{e,b}$ of the algorithms, can be computed by considering the integral of the relation of the converter output power P_o to input power P_i, as expressed bellow:

$$\eta_{e,b} = \frac{\int_{t_1}^{t_2} P_o\, dt}{\int_{t_1}^{t_2} P_i\, dt} \tag{15}$$

Figures 12 through 14 show the simulation results of each MPPT algorithms due to the step variations of the solar radiation, at a reasonably constant cell temperature of 25 ºC. As seen from the case of the P&O algorithm, some tracking errors and oscillations occur specially at higher levels of radiation and startup when compared to IncCond method. The IncCond method proves to be superior to the P&O method in following the MPP of the system. However it also presents troubles at startup. For the case of the proposed MPPT algorithm, simulations demonstrate the highest accuracy of the method, eliminating the oscillations in steady-state without worsening the transient response of the

system. As can be drawn from the instantaneous duty cycle evolution, the adaptive perturbation step reduces the excursions of this parameter and the PV array power error (P_A/P_{max}). In Table II, a summary of the energy efficiency achieved with each MPPT method, including that related to the boost converter is presented. As is noticeable, there is an increase in the efficiency reached by the proposed MPPT algorithm because of its ability to overcome the P&O and IncCond algorithm drawbacks, as following rapid climatic changes and avoiding oscillations around the MPP.

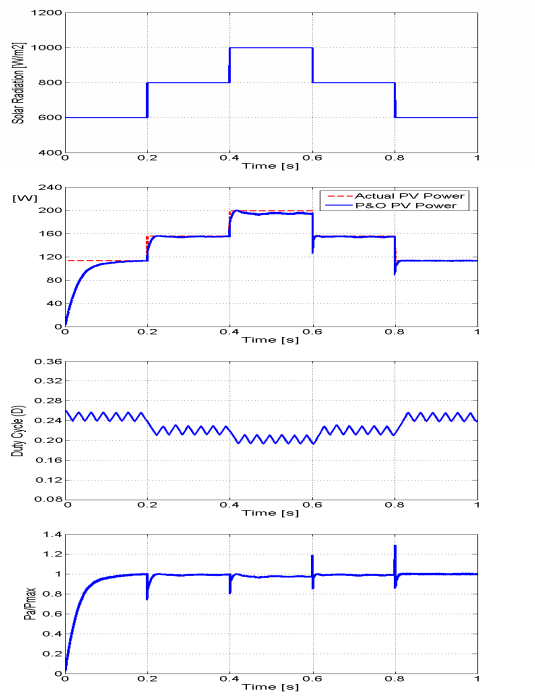

Fig. 12. Simulation results of P&O MPPT algorithm.

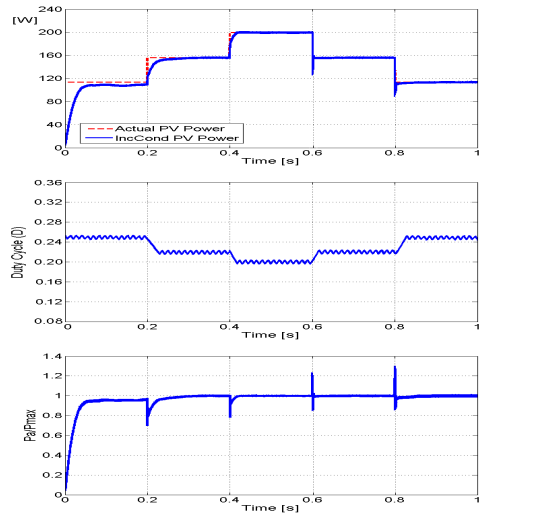

Fig. 13. Simulation results of IncCond MPPT algorithm.

C. Experimental Evaluation

A 200 W laboratory-scale prototype was constructed at the IEE/UNSJ laboratory in order to analyze the actual performance of the PV energy conversion system. The proposed algorithm was implemented by using a high-performance digital signal processor (TMS320F2812) which allows obtaining very small duty cycle perturbation steps. The experimental time domain waveforms of the maximum power drawn from the PV system for different levels of solar radiations was tested through data acquisitions during a clear day for an almost constant cell temperature, as depicted in Figure 15. As can be realized, the MPPT algorithm follows accurately the maximum power that is proportional to the solar radiation. However, a small delay (about 65 ms) arises as a consequence of the digital and analog low pass filter implemented for measuring the voltage and current input quantities.

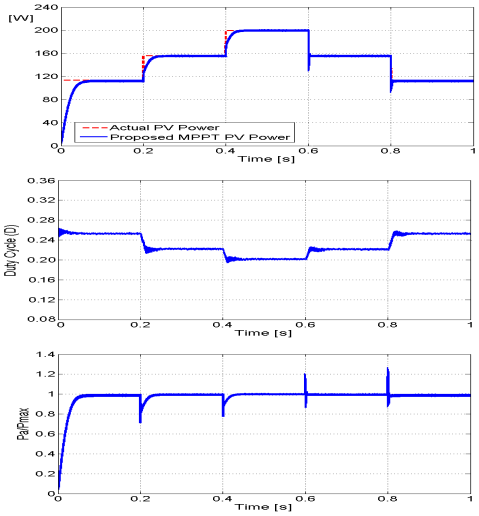

Fig. 14. Simulation results of Proposed MPPT algorithm.

TABLE II
Efficiency comparison among MPP algorithms

MPP Algorithm	MPPT Efficiency, $\eta_{e,PV}$	Boost Converter Efficiency, $\eta_{e,b}$
P&O	96.02	97.04
IncCond	97.10	97.97
Proposed Algorithm	98.01	98.12

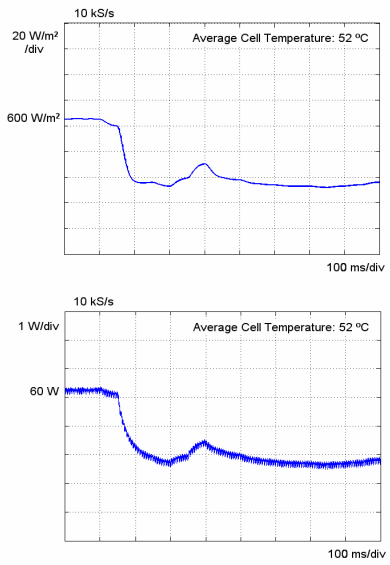

Fig. 15. Experimental results of Proposed MPPT algorithm.

VI. CONCLUSION

In this paper, different techniques for tracking the maximum power point of PV arrays were analyzed and a new MPPT control algorithm based on an enhanced incremental conductance method was proposed in order to improve the efficiency of the PV power generation system at different climatic and load conditions. Both digital simulations and experimental results clearly show the superior performance of the proposed technique with an average efficiency of about 98% in tracking the maximum available PV power for the example presented. Since the algorithm was developed for grid-connected PV applications that typically use a digital controller for implementing all control laws (a DSP in this work), it can be noted that additional hardware requirements are not necessary. It makes the algorithm more cost-effective than other ones.

APPENDIX

The dc/dc boost converter has been designed according to [9] and the specifications stated in Table III.

TABLE III
Dc-dc converter design specifications and components

Specifications and components	Values
Switching frequency	10 kHz
Dc bus voltage (chopper output voltage)	85 V
Chopper input voltage	54.8 – 69.2 V
Chopper duty cycle variation	0 – 0.39
Inductance L_b	13.5 mH
Capacitance C_A (PV array side)	150 μF
Capacitance C (dc bus side)	4.4 mF

REFERENCES

[1] K. Y. Khouzam: "Optimum load matching in direct-coupled photovoltaic power systems - application to resistive loads", *IEEE Trans. on Energy Conv.*, no. 2, pp. 265-271, June 1990.

[2] J. Applebaum, "The quality of load matching in a direct-coupling photovoltaic system", *IEEE Transactions on Energy Conversion*, vol. 2, no. 4, pp. 534-541, Dec. 1987.

[3] S. M. Alghuwainem, "Matching of a DC motor to a photovoltaic generator using a step-up converter with a current locked loop", *IEEE Transactions on Energy Conversion*, vol. 9, NO. 1, pp. 192-198, March 1994.

[4] M. M. Saied, A. A. Hanafy, M. A. El-Gabaly, and A. M. Sharaf, "Optimal design parameter for a PV array coupled to a DC motor via a DC-DC transformer," *IEEE Transactions on Energy Conversion*, vol. 6, pp. 593-598, 1991.

[5] J. Enslin, M. S. Wolf, D. B. Snyman, and W. Sweigers, "Integrated photovoltaic maximum power point tracking converter," *IEEE Transactions on Industrial Electronics*, vol. 44, pp. 769-773, Dec. 1997.

[6] T. Hiyama, S. Kouzuma, and T. Imakubo, "Identification of optimal operation point of PV modules using neural network for real time maximum power tracking control," *IEEE Trans. on Energy Conversion*, vol. 10, no. 3, pp. 360-367, Jn. 1995.

[7] T. Hiyama, S. Kouzuma, T. Imakubo, and T. H. Ortmeyer. "Evaluation of neural network based real time maximum power tracking controller for PV system," *IEEE Trans. on Energy Conversion*, vol. 10, no. 3, pp. 543-548, Sept. 1995.

[8] C. Y. Won, D.-H. Kim and S.-C. Kim, "A new maximum power point tracker of photovoltaic arrays using fuzzy controller", *in Proc. of Power Electronic Specialist Conference,* 396-403, 1994.

[9] J. L. Santos, F. Antunes, A. C. Cícero Cruz, "A maximum power point tracker for PV systems using a high performance boost converter", *Solar Energy*, vol. 80, pp. 772-778, 2006.

[10] C. Hua, J. Lin and C. Shen, "Implementation of a DSP-controlled photovoltaic system with peak power tracking," *IEEE Transactions on Industrial Electronics*, vol. 45, no. 1, pp. 99-107, Feb. 1998.

[11] K. H. Hussein, I. Muta, T. Hoshino, and M. Osakada, "Maximum photovoltaic power tracking: An algorithm for rapidly changing atmospheric conditions," *Proc. IEE-Generation, Transmission and Distribution*, vol. 10, no. 1, pp. 59-64, Jan. 1995.

[12] S. W. Angrist, *Direct energy conversion*, Allyn and Bacon, 2ª Edition, Boston, 1971.

[13] MATLAB/Simulink®, Users´ Guide, MathWorks Inc.

[14] M. G. Molina, and P. E. Mercado, "Control Design and Simulation of DSTATCOM with Energy Storage for Power Quality Improvements", *in Proc. IEEE/PES Transmission and Distribution Latin America*, 01-07, Aug. 2006.

[15] N. Femia, G. Petrone. G. Spagnuolo. M. Vitelli: "Increasing the efficiency of P&O MPPT by converter dynamic matching", *in Proc. IEEE International Symposium on Industrial Electronics, pp. 1-8*, 2004.

BIOGRAPHIES

Marcelo G. Molina was born in San Juan, Argentina, on April 12, 1973. He graduated as Electronic Engineer from the National University of San Juan (UNSJ), Argentina in 1997, and received the Ph.D. degree from the UNSJ in 2004. During 2004, he did part of his doctorate in the Federal University of Rio de Janeiro (UFRJ), Brazil. Since 2004, Dr. Molina is an Associate Professor of Electrical Engineering (IEE/UNSJ) and Researcher of the CONICET. His research interests include simulation methods, power systems dynamics and control, power electronics modeling and design, and the application of energy storage in power systems. Dr. Molina is a Member of the IEEE Power Eng. and Power Electronics Societies.

Domingo H. Pontoriero was born in San Juan, Argentina, on November 3, 1954. He graduated as Electromechanical Engineer from the UNSJ, Argentina in 1980. Eng. Pontoriero is currently Associate Professor of Electrical Engineering at the UNSJ and Researcher of the IEE/UNSJ. His research activities focus on dynamic simulation, power electronics, photovoltaic energy conversion systems and control of electric power systems.

Pedro E. Mercado was born in San Juan, Argentina, on August 26, 1953. He graduated as electromechanical engineer from the UNSJ, and received his Ph.D. from the Aachen University of Technology, Germany. Dr. Mercado is currently Professor of Electrical Engineering at the UNSJ and Researcher of the CONICET. His research activities focus on dynamic simulation, operation security, power electronics, economic operation and control of electric power systems. Dr. Mercado is a Senior Member of the IEEE Power Engineering Society.